Analysis of a soft-x-ray laser with charge-exchange excitation*

William H. Louisell† and Marlan O. Scully‡
Department of Physics and Optical Sciences Center, University of Arizona, Tucson, Arizona 85721

William B. McKnight§
Missile Research, Development and Engineering Laboratory, U.S. Army Missile Command, Redstone Arsenal, Alabama 35809

(Received 9 February 1973; revised manuscript received 4 November 1974)

A soft-x-ray laser utilizing electron pickup by a stripped nucleus is proposed. A particular example using electron exchange between hydrogen and an α particle is analyzed and is shown to produce inversion between the He^{+}_{2p} and He^{+}_{1s} levels giving stimulated emission at 304 Å. In this scheme the α particles are swept along the target at the speed of light. The cross sections involved in the electron pickup in a hydrogen target and subsequent collisional deexcitation are analyzed to ascertain the optimum target thickness for population inversion. Also the effects of atomic collisions on the stimulated-emission cross section are estimated (Doppler broadening). The dynamics of the beam including focusing and space-charge effects are discussed. The stimulated-emission cross sections for a gas and a solid thin-film target are calculated. For a 30-mA α-particle current and a 10-cm lasing length, we estimate gains of 1.1 and 50, respectively.

I. INTRODUCTION

There has been considerable interest in recent years in obtaining laser action in the x-ray frequency region.[1] Recently, several workers have discussed various schemes for x-ray lasers. Lax and Guenther[2] proposed obtaining a population inversion by using a focused mode-locked Nd:glass laser at a power level $\geq 10^{12}$ W on solid low-Z targets. The intense pulsed laser field causes tunneling of valence electrons into the conduction band. In turn, these electrons in the plasma are accelerated and ionize the core electrons, leaving inner-shell vacancies and therefore a population inversion. The experiment of Kepros, Eyring, and Cagle[3] contained in its original inception the notion of a laser-induced plasma "swept" at the velocity of light, producing vacancies in the inner shell of Cu atoms. The work of McCorkle[4] proposes to pass an ion beam through a thin target (e.g., $A^{+}+C \rightarrow A^{++}+C^{*}$). Because of the large cross sections for the selective production of inner-shell vacancies in the ions (or atoms), a population inversion could be achieved. The ion beam is swept along the foil at the velocity of light. A major difficulty with this scheme seems to be the extremely short lifetimes of the inverted population due to Auger processes.

In the present paper we analyze a new proposal for the production of a soft-x-ray laser. The present scheme involves passing a focused collimated beam[5] of completely stripped nuclei (such as He^{++}) through a target (such as solid molecular hydrogen or a confined jet[6] of hydrogen gas) so as to effect selective electron pickup in an excited state. For example, in the case of He^{++} in a hydrogen target, the electron pickup goes mostly (at about 25-keV ion energy) as

$$He^{++}+H_{1s} \rightarrow He^{+}_{2p}+H^{+}, \tag{1.1}$$

since the cross section for pickup in the $2p$ state is larger than for the $1s$ state of He^{+}. This will result in a population inversion between the $2p$ and $1s$ states and stimulated emission of this 304-Å transition is possible. Since the spontaneous decay time,[7] τ_s, is 10^{-10} sec, it is necessary to sweep the ions along the foil at the speed of light. In this way, radiation emitted from the first ions can stimulate radiation from inverted ions arriving along the foil later. This may be accomplished in several ways. The present scheme for stimulated emission of soft x rays is attractive in its simplicity and its extension to shorter wavelengths is feasible. The largest source of uncertainty in assessing the feasibility of the scheme lies in the lack of adequate cross-section measurements used in the calculation. (See, however, note added in manuscript, Ref. 8.)

II. BEAM SWEEP, TARGETS, AND POPULATION INVERSION

There are several ways one might sweep the ions along a target at the speed of light. The most obvious way is to pass the beam between a pair of deflection plates to which is applied a time-varying voltage. If we place a target downstream beyond the deflection plates and transverse to the original beam direction, the beam may be swept along the target at the velocity of light. There are at least two difficulties with this method. Since the beam will have different velocity components parallel to the target (and the lasing direction) as

different ions strike, there will be a large Doppler shift with consequent loss in gain. However, it is found on further analysis that a factor of c/v_0 is lost in the gain (v_0 is the longitudinal beam velocity) compared with other deflection schemes.

An alternative arrangement is to have the target again downstream beyond the deflection plates, but parallel to the plates. This geometry has several advantages (e.g., it eliminates Doppler broadening associated with the transverse beam emittance, improves the gain over the above scheme by a factor c/v_0, etc.) and will be discussed in a later publication.

A third possibility is a modification of McCorkle's proposal which we shall analyze below. This scheme, as well as the two mentioned above, suffers because rather large ion densities are needed at the target to produce adequate gain. Space charge as well as the ion-beam emittance limit the size to which a given ion beam may be focused. However, detailed (numerical) beam-transport analysis[9] indicates that the ion densities required to produce an adequate population inversion are possible using currently available ion sources. For simplicity, we shall neglect such considerations in the present paper and they will be considered in detail in a later publication. We analyze the modified McCorkle scheme for several reasons. Firstly, there are several possible ways to overcome the space-charge effects. Secondly, the first impression one gets of the beam dynamics of this sweep scheme is that the beam hits the target like water from a hose which is swept along the target. This is incorrect and results in a calculated gain/cm which is in error by a factor c/v_0. In reality, the entire beam is swept up to the target rigidly, but tilted at a small angle (v_0/c) with respect to the initial beam direction so that the area of intersection of the beam with the target is completely different from the "water-hose" picture. Thirdly, many of the results obtained here will be useful for other schemes we shall consider. With these objectives in mind and armed with the foreknowledge that alternate "more practical" schemes are possible (which we shall discuss elsewhere) and which lead to similar results (with the c/v_0 factor correction), we proceed with the present study.

A well-focused collimated He^{++} ion beam travels along the z axis between the plates of a parallel-plate transmission line of length L and spacing d as shown in Fig. 1. A pulsed electric field $E_x = E_0 u[z + c(t - t_0) - L]$, where $u(\xi)$ is the unit step function, is applied at $z = L$ at time t_0, and travels upstream to $z = 0$ with velocity c. In the upper plate is a slot of width Δy and length l which allows the ions to exit a definite distance behind the advancing wave front. (In the McCorkle scheme, the target is placed in the slot in the upper plate.) Beyond the upper plate the ions enter a field-free drift region in which we might, for example, space-charge neutralize the ions to allow a "focusing" of the beam. The target, as seen in Fig. 1, is placed parallel to the deflection plates and a distance b above it. By choosing this plate-target separation properly, ions which were originally at the bottom of the beam on entry (at $x_0 = -\frac{1}{2}\epsilon$) can be made to hit the foil at the same time as the ions originally at the top of the beam on entry ($x_0 = +\frac{1}{2}\epsilon$). This is because those at $x_0 = -\frac{1}{2}\epsilon$ exit with a greater velocity than those from $x_0 = +\frac{1}{2}\epsilon$. This prevents any loss of potential excitation current due to having some ions arrive at the target with a time separation greater than τ_s and has a focusing effect. In addition, by having the target above, the radiation will be farther removed from the direction of the ion source. Again the excitation is swept along the target at the velocity c in the upstream direction. As noted above, alternative focusing schemes will be discussed elsewhere.

We shall consider two different electron-pickup arrangements. The first will consist of a solid molecular hydrogen target of thickness δ. We find

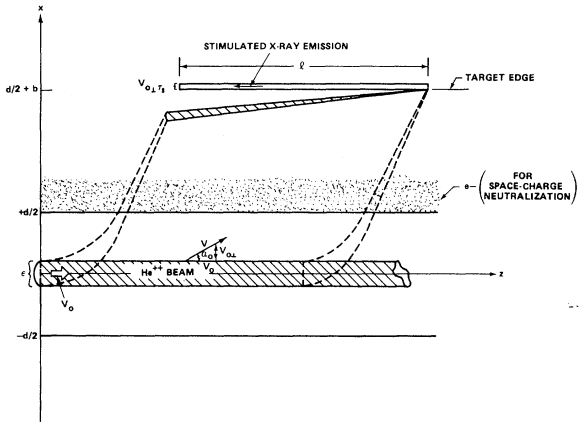

FIG. 1. Possible deflection, pumping, and focusing arrangement for obtaining x-ray laser action. A focused He^{++} beam travels to the right with velocity v_0 between the plates of a strip transmission line with separation d. A pulse of amplitude $E_0 = V_d/d$ is launched on the line from the downstream end which travels to the left at the velocity of light and deflects the ions upward. The last ion reaches the upper plate (and the target) at a time l/c later than the first ion separated by a distance l from it. A small slot in the upper plate allows the ions to enter a drift region and strike a hydrogen-gas-jet target a distance b above the upper plate. We show the focused beam just as the first ion strikes the target. Lasing occurs in the upstream direction.

that the thickness which maximizes electron pickup in the $2p$ state as opposed to competing processes is such that $\delta \ll V_0\tau_s$, where V_0 is the ion velocity in the target. This has the advantage that the "pumped" ions exit from the target before radiating and there is no absorption of the x rays in the target. However, this scheme has several disadvantages. The foil thickness needed to maximize inversion is so thin that such foils will be difficult to make, yet they are thick enough so that competing processes such as double-electron pickup, de-excitation collisions, multiple scattering, etc., are sufficient to cause some reduction in gain. In addition, the foils will be destroyed by the ions.

To eliminate these difficulties, we shall also consider a target which consists of a gas jet of atomic or molecular hydrogen. We adjust its density to maximize one electron pickup in the $2p$ state in a spontaneous decay length, $V_0\tau_s$. It is found that for the optimum density, multiple scattering and other competing processes are reduced with a net gain enhancement over the solid target. In addition, we do not have the complication of making thin foils, and repetitive pulse operation becomes possible. One minor disadvantage is that there is a small amount of x-ray absorption in the gas, but it appears negligible[10] at the optimum density. We proceed to analyze the above scheme in more detail.

We first calculate the number of excess ions in the $2p$ state per unit volume which exist at a particular instant of time on traversing the target. Let i be the total He^{++} ion current entering the transmission line. Then $i/2e$, where $e = +1.6\times10^{-19}$ C, will be the number of He^{++} ions/sec which cross a given plane. These are swept up by the pulse to the target region. In traversing the target, a fraction ΔP excess $2p$ He^{+} ions are created. If v_0 is the longitudinal velocity, then in a spontaneous lifetime the total excess number of excited ions is $ic\tau_s/2ev_0$. They occupy a volume $\Delta y(c\tau_s)(V_{0\perp}\tau_s) \equiv \Delta x\Delta y c\tau_s$, where Δx and Δy are the excited beam widths in the x and y dimensions, respectively, and $V_{0\perp}$ is the ion velocity transverse to the target so that the excess population density is

$$N(r_{2p} - r_{1s}) \equiv i\Delta P/2ev_0\Delta x\Delta y, \tag{2.1}$$

where N is the total number of ions and r_{2p} and r_{1s} are the rates which ions are created in the $2p$ and $1s$ states, respectively.

III. BEAM DYNAMICS

A pulse is launched on a transmission line from $z = L$ at time t_0 given by

$$E_x = E_0 u[z + c(t - t_0) - L], \tag{3.1}$$

where $u(\xi)$ is the unit step function. It travels upstream with velocity c. The ith He^{++} ion enters the transmission line at time t_i with velocity v in the z direction so that for $t > t_i$,

$$z_i = v(t - t_i). \tag{3.2}$$

This ion meets the leading edge of the pulse at time t_{im} given by

$$t_{im} = (L + vt_i + ct_0)/(c + v). \tag{3.3}$$

The acceleration in the x direction for $t > t_{im}$ is given by

$$\frac{d^2x_i}{dt^2} = \frac{eE_0}{2M} \equiv a, \tag{3.4}$$

where the proton mass $M = 1.67\times10^{-27}$ kg. The velocity and position for $t > t_{im}$ are

$$dx_i/dt = a(t - t_{im}), \tag{3.5}$$

$$x_i = x_0 + \tfrac{1}{2}a(t - t_{im})^2, \tag{3.6}$$

where x_0 is the x coordinate of ion i on entering. For simplicity, we neglect any initial velocity in the x direction.

At time t_{ie}, ion i reaches the slot in the upper plate located at $x_i(t_{ie}) \equiv x_e = \frac{1}{2}d$ and exits. This time is given by

$$t_{ie} = t_{im} + \{(2Md/eE_0)[1 - (2x_0/d)]\}^{1/2}. \tag{3.7}$$

The square-root term is the time it takes the ion to reach the upper plate after it meets the pulse. When the ion exits its longitudinal position is given by

$$z_i(t_{ie}) \equiv z_{ie} = \frac{v}{c + v}[L + c(t_0 - t_i)] + \frac{d}{\alpha}\left(1 - \frac{2x_0}{d}\right)^{1/2}, \tag{3.8}$$

where

$$\alpha \equiv (eE_0d/2Mv^2)^{1/2}. \tag{3.9}$$

We may alternately express t_i in terms of t_{ie} from (3.7) and (3.3) and reexpress (3.8) as

$$z_{ie} = -ct_{ie} + L + ct_0 + (c + v)(d/v\alpha) \times [1 - (2x_0/d)]^{1/2}, \tag{3.10}$$

which shows that $\delta z_{ie}/\delta t_{ie} = -c$, so that ions are swept along the upper plate at velocity c in the upstream direction.

Consider now ions entering with velocity $v = v_0$ located at $x_0 = 0$. To utilize the pulse most efficiently, we would like the first ions to exit at $z_{ie} = L$. From (3.8) this requires that they enter at time t_1 given by

$$L + c(t_0 - t_1) = [(c + v_0)/v_0]\,[L - (d/\alpha_0)], \tag{3.11}$$

where

$$\tan\theta_0 \equiv \alpha_0 \equiv (eE_0 d/2Mv_0^2)^{1/2}. \tag{3.12}$$

We would like the last ions to enter at the time the pulse reaches $z = 0$. This requires that t_l be given by

$$L + c(t_0 - t_l) = 0. \tag{3.13}$$

These ions, by (3.8), exit at

$$z_{le} = d/\alpha_0 \equiv L - l, \tag{3.14}$$

which defines l. If we use this in (3.11), we obtain

$$L + c(t_0 - t_1) = (c + v_0)l/v_0. \tag{3.15}$$

All ions which enter with $t_i > t_l$ will exit at the same z_{le} and will not be swept with velocity c. The useful ions enter then between t_l and t_1, which by (3.13) and (3.15) is given by

$$t_l - t_1 = (c + v_0)l/cv_0. \tag{3.16}$$

From (3.13) and (3.15), we may parametrize the particles entering between t_1 and t_l by T, where

$$L + c(t_0 - t_i) \equiv T(c + v_0)l/v_0. \tag{3.17}$$

Here $T = 1$ for ions that enter at t_1, and $T = 0$ for ions that enter at t_l. With this notation we may write (3.7) and (3.8) as

$$t_e(v, x_0, T) = t_0 + \frac{L}{c} - T\left(\frac{v}{v_0}\right)\frac{c + v_0}{c + v}\,\frac{l}{c} + \{(2Md/eE_0)[1 - (2x_0/d)]\}^{1/2} \tag{3.18}$$

and

$$z_e(v, x_0, T) = T\left(\frac{v}{v_0}\right)\left(\frac{c + v_0}{c + v}\right) l + (d/\alpha)[1 - (2x_0/d)]^{1/2}. \tag{3.19}$$

Further, the velocity in the z direction when the ion exits is unchanged ($dz_e/dt = v$) while in the x direction it is (Fig. 2)

$$\frac{dx_e}{dt} = v\alpha\left[1 - \left(\frac{2x_0}{d}\right)\right]^{1/2} \equiv V\sin\theta_e = v\tan\theta_e. \tag{3.20}$$

The magnitude of the velocity when the ion exits is

$$V = v\{1 + \alpha^2[1 - (2x_0/d)]\}^{1/2}. \tag{3.21}$$

The beam energy per ion when it exits is

$$U_e = 2MV^2 = 2Mv^2 + eE_0 d[1 - (2x_0/d)]. \tag{3.22}$$

Since this energy is not changed either in the case of a field-free drift region or in a uniform magnetic field region, this is the ion energy on entering the pump region. For particles with entering velocity $v = v_0$ on axis at $x_0 = 0$, we have

$$U_0 = 2MV_0^2 = 2Mv_0^2 + eE_0 d = 2Mv_0^2(1 + \alpha_0^2). \tag{3.23}$$

Also we have that the pulse voltage needed is

$$eE_0 d = U_0\alpha_0^2/(1 + \alpha_0^2). \tag{3.24}$$

The beam now passes through a slot in the upper plate of length l and width Δy into a field-free region. The ions travel in the field-free region with unchanged velocity and their positions are given by ($t > t_e$)

$$x_i = \tfrac{1}{2}d + (dx_e/dt)(t - t_e), \tag{3.25}$$

$$z_i = z_e + v(t - t_e). \tag{3.26}$$

At $x_{ih} = b + \frac{1}{2}d$, the ions hit the pump region at time t_h given by

$$t_h = t_e + b\Big/\frac{dx_e}{dt}, \tag{3.27}$$

and their position on the target is

$$z_h = z_e + \left(vb\Big/\frac{dx_e}{dt}\right). \tag{3.28}$$

Their angle is unchanged as is their z component of velocity. As a result, all Doppler broadening that exists when the ions hit the pump region is due to the initial velocity spread in the beam when it enters the system.

IV. EFFECTS OF VELOCITY SPREAD AND BEAM THICKNESS

We assume the beam has a velocity spread of $\delta v_0 \ll v_0$ and thickness $\delta x_0 = \epsilon$ when it enters. From Eqs. (3.18)–(3.20) and (3.25)–(3.28), we obtain

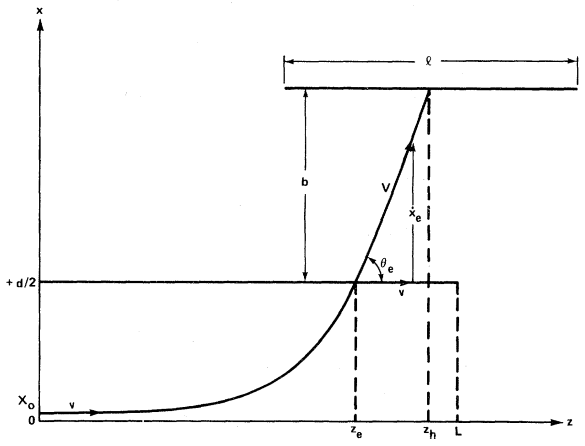

FIG. 2. Path of ion in deflection and drift region.

$$z_h = -ct_h + ct_0 + L + \left(1 + \frac{c}{v}\right)\alpha^{-1} \times \left[b\left(1 - \frac{2x_0}{d}\right)^{-1/2} + d\left(1 - \frac{2x_0}{d}\right)^{1/2}\right], \quad (4.1)$$

so that ions still sweep the target at velocity $\delta z_h/\delta t_h = -c$. Also we have that

$$t_h = t_0 + \frac{L}{c} - T\left(\frac{v}{v_0}\right)\left(\frac{c+v_0}{c+v}\right)\frac{l}{c} + \alpha^{-1}v^{-1}\left[b\left(1 - \frac{2x_0}{d}\right)^{-1/2} + d\left(1 - \frac{2x_0}{d}\right)^{1/2}\right]. \quad (4.2)$$

For ions with velocity v_0, we easily see that if we let $b = d[1 - (\epsilon/d)^2]^{1/2}$, ions from $x_0 = -\frac{1}{2}\epsilon$ will hit the target at the same time as ions from $x_0 = +\frac{1}{2}\epsilon$. In addition, they all hit at the same position on the target. That is, the x dimension of the beam is focused on the target. There is, of course, no focusing as yet in the y direction which could be accomplished in several ways. Space-charge repulsion will tend to counteract this focusing. However, in recent calculations[9] (on other sweep schemes combined with focusing), it has been found that (~25 mA) beam emittance rather than space charge is the limiting consideration. We will assume, for the purpose of the present discussion, that some means of space-charge neutralization in the drift region has been realized and ignore space-charge effects.[11] The effective beam volume will then be determined by the geometry and the method used to neutralize space charge as well as the decay of the population inversion. The variation in arrival time due to the velocity spread is seen to be

$$|\delta t_h| = (\delta v_0/v_0)[Tl/(c+v_0)], \quad (4.3)$$

which will be short compared with the spontaneous lifetime as we shall see.

We consider now a special set of design parameters. The cross section[12-15] for electron pickup in the $2p$ state of He^+ is a maximum at 25 keV. The Doppler broadening when the ions hit the target is given by

$$\Delta\omega_D = (\omega/c)\delta v_0 = 2\pi\delta v_0/\lambda, \quad (4.4)$$

and for a spread in source energy δE, we have

$$\delta v_0 = \tfrac{1}{2}(\delta E/E)v_0.$$

The ion beams involved[5] have an energy spread $\delta E \simeq 1$ eV which implies $\Delta\omega_D = 4\times10^9$ sec^{-1}, which is also negligible compared with Doppler broadening due to scattering in the target as we shall see later.

V. PUMP REGION

To determine the optimum target thickness δ for $2p$ pickup, we first consider some of the electron pickup processes that occur as a He^{++} ion traverses either a solid-hydrogen foil or a thin jet of hydrogen atoms or molecules. Let a refer to the $2p$ state and b to the $1s$ state of He^+. Let $P_{00}(x)$ be the probability of having a He^{++} ion at x, $P_{\alpha 0}(x)$ the probability of having one electron in any state α of He^+, and $P_{\alpha\beta}(x)$ the probability of having two electrons, one in state α and another in state β. The number of He^{++} ions will decrease as it goes through the pickup regions if it picks up either one or two electrons. The number will increase if one or more electrons are stripped off a He^+_α or $He_{\alpha\beta}$. Since the cross section for capturing one electron is larger than for capturing two or for stripping, we have approximately

$$\frac{dP_{00}}{dx} \cong -\sum_\alpha \lambda_\alpha P_{00} \equiv -\lambda P_{00}, \quad (5.1)$$

where the inverse mean free path is

$$\lambda_\alpha = \sigma_\alpha N_f, \quad (5.2)$$

and σ_α is the cross section for the process

$$He^{++} + H \rightarrow He^+_\alpha + H^+, \quad (5.3)$$

and N_f is the number of atoms/cm^3 in the target region.

Let us estimate the σ_α's. Unfortunately, the calculations of Schiff,[14] Coleman and McDowell,[13] and McElroy[12] are not too reliable at 25 keV. In Table I, we list some of their results. Furthermore, the lowest energies studied experimentally by Fite *et al.*[16] only go up to about 40 keV which makes comparison of theory and experiment difficult. In addition Fite *et al.* measured only σ (total). Pending calculations of the Landau-Zener[15] type, we shall therefore settle for the approximate values

$$\sigma(2p_z) \cong 100\times10^{-17} \text{ cm}^2/\text{atom},$$
$$\sigma(1s) \cong 1\times10^{-17} \text{ cm}^2/\text{atom}, \quad (5.4)$$
$$\sigma(\text{total}) \cong 500\times10^{-17} \text{ cm}^2/\text{atom}.$$

We also have the question of molecular versus atomic cross sections since in the case of solid targets, we have molecular hydrogen whereas in the hydrogen gas jet, we may have atomic hydrogen. Following the Tuan and Gerjuoy[17] philosophy and taking a molecular atomic binding limit with corresponding $Z_{\text{eff}} \sim 1.2$, we find $\sigma_2(\text{mol}) \cong 300\pi a_0^2$ (where $a_0 = 0.524\times10^{-8}$ cm) as compared with the early Brinkman-Kramers[18] (BK) atomic value of $600\pi a_0^2$ and $\sigma_1(\text{mol}) \cong 0.3\pi a_0^2$ as compared with $\sigma_1(\text{at}) \cong 0.03\pi a_0^2$. Also $\sigma_T(\text{mol}) \cong 450\pi a_0^2$ as compared with $\sigma_T^{\text{BK}}(\text{at}) \cong 900\pi a_0^2$. Thus, $\sigma(\text{mol}) \cong 2\sigma(\text{at})$. Also

σ(mol) and σ(at) give approximately the same ratio for $(\sigma_2 - \sigma_1)/\sigma_T \cong 0.3$ and thus yield about the same population inversion.

In the case of solid molecular hydrogen with a density of about 4×10^{22} atoms/cm^3, we have from (5.2) and (5.4),

$$\lambda_{2p} \cong 400\times10^5 \text{ cm}^{-1},$$
$$\lambda_{1s} \cong 4\times10^5 \text{ cm}^{-1} \tag{5.5}$$
$$\lambda \cong 2000\times10^5 \text{ cm}^{-1}.$$

In the case of the atomic-hydrogen jet with a density of approximately 0.5×10^{17} atoms/cm^3, we have

$$\lambda_{2p} \cong 50 \text{ cm}^{-1}, \quad \lambda_{1s} \cong 0.5 \text{ cm}^{-1},$$
$$\lambda \cong 250 \text{ cm}^{-1}. \tag{5.6}$$

This corresponds to a pickup length (λ_{2p}^{-1}) for $2p$ pickup equal approximately to one spontaneous decay length $V_{0\perp}\tau_s$.

Next we consider the change in the number of He_α^+ ions in traversing the target. We have

$$\frac{dP_{\alpha0}}{dx} \cong \lambda_\alpha P_{00}(x) - \sum_{\beta\neq\alpha}(\gamma_\alpha^\beta + \Lambda_\alpha^\beta)P_{\alpha0} + \sum_{\beta\neq\alpha}\gamma_\beta^\alpha P_{\beta0}, \tag{5.7}$$

where, from (5.1),

$$P_{00}(x) = e^{-\lambda x}. \tag{5.8}$$

The first term represents the increase due to one electron pickup as indicated in (5.3). The γ_α^β terms represent decay processes associated with one-electron transitions from α to β:

$$He_\alpha^+ + X \to He_\beta^+ + X^*. \tag{5.9}$$

Since our He_α^+ ion is moving with an energy of about 25 keV and the binding of the electron to X is a few electron volts, we may estimate the cross sections for the processes indicated by (5.9) by assuming the electrons and nuclei of X form a plasma.[19] [This would not be a valid picture for the processes in (5.3).] The important process then is

$$He_\alpha^+ + e \to He_\beta^+ + e', \tag{5.10}$$

and we estimate this cross section to be[20]

$$\sigma_{\alpha\beta} \cong 10^{-17} \text{ cm}^2/\text{atom}. \tag{5.11}$$

For the solid targets, we have

$$\gamma_a^b \cong \gamma_b^a = \sigma_{ab}\rho = 4\times10^5 \text{ cm}^{-1} \equiv \gamma, \tag{5.12}$$

and for the gas jet

$$\gamma \cong 0.5 \text{ cm}^{-1}. \tag{5.13}$$

The last terms in (5.7), $\sum\gamma_\beta^\alpha P_{\beta0}$, represent transitions back to state α.

The terms $-\sum_\beta \Lambda_\alpha^\beta P_{\alpha0}$ represent a second electron pickup

$$He^+ + H \to He + H^+, \tag{5.14}$$

which involves a cross section[14] of 8.5×10^{-17} cm^2/atom; therefore, for the solid target we have

$$\Lambda \cong \sum_\beta \Lambda_\alpha^\beta \cong 3.6\times10^6 \text{ cm}^{-1}, \tag{5.15}$$

while for the gas jet,

$$\Lambda \cong 4.3 \text{ cm}^{-1}. \tag{5.16}$$

This is an important competing process. Other processes not given in (5.7) are negligible.

Finally, for the solid target the inverse radiative decay length is of order $(V_{0\perp}\tau_s)^{-1} \sim 10^2$ cm^{-1} and is negligible. However, it is significant for the gas jet so that γ becomes

$$\gamma \cong 100 \text{ cm}^{-1} \tag{5.17}$$

instead of the value given in (5.13).

With these approximate values, (5.7) reduces to

$$\frac{dP_{\alpha0}}{dx} \cong \lambda_\alpha e^{-\lambda x} - (\Lambda+\gamma)P_{\alpha0} + \gamma P_{\beta0}, \tag{5.18}$$

where $\alpha = a \equiv 2p$ and $\beta = b \equiv 1s$ or vice versa. Thus, the principal processes are one- and two-electron capture and transitions between the $1s$ and $2p_z$ states. At $x = 0$ we have that $P_{\alpha0}(0) = 0$ and we easily see that the population difference is

TABLE I. Cross sections in units of 10^{-17} cm^2/atom for processes (5.3).

	McElroy[a] (25 keV)	McElroy[a] (100 keV)	Schiff[b] (100 keV)	Coleman and McDowell[c]
$\sigma(1s)$	2.8	5.96	15	0.4
$\sigma(2s)$	35.0	10.7	75	500.0
$\sigma(2p_x)$	55.1	18.1	75	500.0
$\sigma(2p_z)$	68.4	30.5	75	500.0
σ(total)	246.0	154.0	200	1900.0
$(\sigma_{2p_z} - \sigma_{1s})/\sigma_T$	0.27	0.16	0.3	0.26

[a]Reference 12. [b]Reference 14. [c]Reference 13.

$$P_a(x) - P_b(x) \equiv \Delta P(x) = \frac{\lambda_a - \lambda_b}{\lambda - \Lambda - 2\gamma} (e^{-(\Lambda+2\gamma)x} - e^{-\lambda x}). \tag{5.19}$$

The population difference is a maximum when the pump region thickness has the value

$$x_{\max} = \frac{\ln[\lambda/(\Lambda+2\gamma)]}{\lambda - \Lambda - 2\gamma} . \tag{5.20}$$

For our solid target, we have

$$x_{\max} \cong 2 \text{ Å}, \tag{5.21}$$

while for the gas jet

$$x_{\max} \cong 4.4 \times 10^{-3} \text{ cm}. \tag{5.22}$$

Since 2 Å is impractical, we have from (5.19) that

$$\Delta P(25 \text{ Å}) \cong 0.1. \tag{5.23}$$

For a gas jet with a thickness[6] of 10^{-2} cm, we have by (5.19)

$$\Delta P(10^{-2}) \cong 0.05. \tag{5.24}$$

Although we have lost a factor of 2 in the gain, the improvement in Doppler broadening is significant as we shall show next.

We have designed our system so that until the ions enter the pump region, Doppler broadening is negligible compared with homogeneous broadening. However, ion-ion scattering in the foil or jet introduces a spread in velocities, Δv_z, in the z direction which cause Doppler broadening.

We first estimate the Doppler broadening for a solid target. The energy added to our He_{2p}^+ ion due to a single screened Coulomb encounter is of order $2e^2/4\pi\epsilon_0 a_0 \cong 20$ eV $= \delta U_0$ for an average impact parameter of $\frac{1}{2}a_0$. The velocity change this causes is then

$$\delta V_0 \cong V_0 \delta U_0 / 2U_0 \cong 4.8 \times 10^4 \text{ cm/sec}. \tag{5.25}$$

For a 25-Å-thick solid target, we should increase this by a factor $\sim(25)^{1/2}$. This leads to a Doppler width of approximately

$$\Delta\omega_D \cong 2\pi\delta V_0/\lambda \lesssim 10^{12} \text{ sec}^{-1}, \tag{5.26}$$

which should be compared with a homogeneous linewidth of 10^{10} sec^{-1}.

Next we estimate the Doppler broadening for a gas target due to a charge-exchange collision. The relative velocity in the lasing direction is given to a good approximation by

$$v(b) = (e^2/4\pi\epsilon_0 \mu v_0 b)\sin\theta_0, \tag{5.27}$$

where θ_0 is the angle the incident ion makes with the target, b is the impact parameter, μ is the He-H reduced mass, and $v_0 \cong 10^8$ cm/sec is the "beam" velocity. If the beam cross section is $\sigma = \pi b_m^2$, it is reasonable to assume that the probability distribution for b is

$$P(b)\,db = \begin{cases} 2\pi b\,db/\pi b_m^2, & b \leq b_m, \\ 0, & b > b_m. \end{cases} \tag{5.28}$$

This gives for the average of v

$$\langle v \rangle = (2e^2/4\pi\epsilon_0 b_m \mu v_0)\sin\theta_0, \tag{5.29}$$

which may be rewritten in terms of the Bohr radius a_0 as

$$\langle v(He^+) \rangle = \frac{e^2}{4\pi\epsilon_0 a_0} \frac{1}{\frac{1}{2}m_2 v_0^2} \frac{a_0}{b_m} v_0 \sin\theta_0 = \frac{26 \text{ eV}}{25 \text{ keV}} \frac{a_0}{b_m} v_0 \sin\theta_0. \tag{5.30}$$

If we let $b_m = 5a_0$ (see Ref. 8), we find

$$\langle v(He^+) \rangle = 2 \times 10^4 \sin\theta_0 \text{ cm/sec}, \tag{5.31}$$

for a Doppler width of

$$\langle \Delta\omega_D \rangle \sim 2 \times 10^{10} \text{ sec}^{-1} \tag{5.32}$$

for $\theta_0 = 30°$.

VI. GAIN: EXAMPLES AND DISCUSSION

In the Appendix we calculate the net linear gain[21] for a solid target in which the Doppler width ($\Delta\omega_D \cong 10^{12}$ sec^{-1}) is much larger than the radiative width ($\Delta\omega_S = 10^{10}$ sec^{-1}). By Eq. (A40),

$$G_{\text{solid}} = \left[\frac{3}{4}\left(\frac{\ln 2}{\pi}\right)^{1/2} \lambda^2 \frac{\Delta\omega_S i \Delta P}{\Delta\omega_D e v_0 \Delta x \Delta y} - 2\kappa\right] l. \tag{6.1a}$$

For a gas target for which $\Delta\omega_D \cong 2 \times 10^{10}$ sec^{-1}, we have by Eq. (A39),

$$G_{\text{gas}} = \left[\frac{3}{4}\left(\frac{\ln 2}{\pi}\right)^{1/2} \lambda^2 \frac{\Delta\omega_S}{\Delta\omega_D} \times \frac{i\Delta P}{e v_0 \Delta x \Delta y} e^{\beta^2}(1 + \text{erf}\beta) - 2\kappa\right] l \tag{6.1b}$$

and

$$\beta = \frac{(\ln 2)^{1/2}(\gamma_a - \gamma_b)}{\Delta\omega_D} \sim \frac{(\ln 2)^{1/2}\Gamma_{ab}}{\Delta\omega_D} . \tag{6.2}$$

Let us consider the maximum lasing length consistent with ignoring diffraction losses. The diffraction angle associated with a source of physical extent $\Delta x = V_{0\perp}\tau_s = v_0\alpha_0\tau_s$ is, of course,

$$\theta = \lambda/\Delta x. \tag{6.3}$$

Radiation from the downstream end of our lasing medium will spread over a distance Δx in a length l_D given by

$$\Delta x = l_D \theta, \tag{6.4}$$

and the maximum (lossless) diffraction length is then given by the familiar expression

$$l_D = (\Delta x)^2/\lambda = V_{0\perp}^2 \tau_s^2/\lambda, \tag{6.5}$$

which, in our case, is approximately 10 cm. We may therefore neglect diffraction losses.

In the case of the hydrogen jet target, there will be some x-ray absorption. The absorption cross section[10] for 300-Å x rays in H is 2.78×10^{-19} cm^2 so that for a gas jet of density 5×10^{16} atoms/cm^3, the loss per cm is

$$\kappa = \sigma N_f \cong 1.39\times10^{-2}\ \text{cm}^{-1}. \tag{6.6}$$

For the $2p$-$1s$ transition in He^+, $\lambda = 3\times10^{-6}$ cm and the spontaneous linewidth $\Delta\omega_S = 10^{10}$ sec^{-1}. For a solid-hydrogen target 25 Å thick, $\Delta\omega_D \cong 10^{12}$ sec^{-1} and $\Delta P = 0.1$. We take for our focused beam $\Delta x = V_{0\perp}\tau_s \cong 5.5\times10^{-3}$ cm and $\Delta y \cong 10^{-2}$ cm. We also have $v_0 = 9.8\times10^7$ cm/sec. The homogeneous linewidth is 10^{10} sec^{-1} so $\gamma_{ab}/\Delta\omega_D \ll 1$ (see the Appendix). For a 30-mA beam 10 cm long, (6.1a) yields a gain of 1.10 for the solid target. For a gas jet, $\Delta P \cong 0.05$ and $\Delta\omega_D \cong 2\times10^{10}$ sec^{-1}, the gain is by (6.1b) 47. By (6.5) we see the absorption is negligible in the gas target. These correspond to $e^{1.1} \cong 3$ and $e^{47} \cong 2.6\times10^{20}$ x-ray quanta, respectively! Of course, this means the linear theory is no longer valid. With the gas target, repetitive pulse operation is possible.

Ion currents in considerable excess (orders of magnitude) of 20 mA from a duoplasmatron[5,22] are readily available. The 25-keV beam energy is dictated by the accidental resonance between the $1s$ state of hydrogen and the $2p$ state of helium where the cross section is a maximum. The focused beam area, $\Delta x\,\Delta y \cong 5.5\times10^{-9}$ m^2, is optimistic but reasonable (as suggested by recent calculations[8]) and could be relaxed due to the large gains. These and other problems will be discussed elsewhere.

ACKNOWLEDGMENTS

The authors would like to acknowledge valuable discussions with J. Bayfield, W. Bickel, J. Brolley, K. Boyer, C. Cantrell, D. Donahue, D. Eccleshall, R. Emigh, J. Garcia, H. Hill, D. Judge, G. Khayrallah, W. Lamb, Jr., E. McDaniel, R. McCorkle, G. Moore, R. Moore, D. Mueller, W. Otto, D. Rogovin, R. Shea, J. Stoner, W. Wing, and P. Wunsch.

APPENDIX: LASER GAIN WITH δ-FUNCTION PUMPING

In the present laser scheme ions are pumped into the $2p$ and $1s$ states as they intersect the target at the velocity of light. In this appendix we calculate the gain for such a δ-function pumping.[21]

We consider a two-level "atom" with states $\alpha = a, b$. The density matrix obeys the equations of motion

$$\partial_t \rho_{aa} = r_a \delta\left(t - \frac{z}{c}\right) - \gamma_a \rho_{aa} - i\left(\frac{\mathcal{P}E}{\hbar}\right)(\rho_{ab} - \rho_{ba}), \tag{A1}$$

$$\partial_t \rho_{bb} = r_b \delta\left(t - \frac{z}{c}\right) - \gamma_b \rho_{bb} + i\left(\frac{\mathcal{P}E}{\hbar}\right)(\rho_{ab} - \rho_{ba}), \tag{A2}$$

$$\partial_t \rho_{ab} = -(i\omega + \Gamma_{ab})\rho_{ab} - i\left(\frac{\mathcal{P}E}{\hbar}\right)(\rho_{aa} - \rho_{bb}), \tag{A3}$$

$$\rho_{ba} = \rho_{ab}^* . \tag{A4}$$

Here r_α is the fraction of the number of "atoms" pumped into level α, $\mathcal{P}$ is the dipole matrix element between states a and b, $E(z, t)$ is the electric field, γ_α represent the atomic decay rates for level α, $\Gamma_{ab} = \frac{1}{2}(\gamma_a + \gamma_b) + \Gamma_{ab}^{\text{ph}}$, and $\hbar\omega = \epsilon_a - \epsilon_b$ gives the energy-level separation between levels a and b.

The macroscopic polarization is given by

$$P(z, t) = N\mathcal{P}\int_{-\infty}^{\infty} d\omega\, \sigma(\omega) \times [\rho_{ab}(z, t, \omega) + \rho_{ba}(z, t, \omega)], \tag{A5}$$

where N is the number of "atoms" per unit volume and $\sigma(\omega)$ is the atomic distribution, which for Doppler broadening we take as the Gaussian

$$\sigma(\omega) = \sigma_0 e^{-[4\ln 2(\omega-\nu)^2/(\Delta\omega_D)^2]},$$
$$\sigma_0 = (2/\Delta\omega_D)(\ln 2/\pi)^{1/2}, \tag{A6}$$

where $\Delta\omega_D$ is the full Doppler linewidth at half-maximum.

The electric field obeys the wave equation

$$\frac{\partial^2 E}{\partial z^2} - \frac{1}{c^2}\frac{\partial^2 E}{\partial t^2} - \mu_0\sigma\frac{\partial E}{\partial t} = \mu_0\frac{\partial^2 P}{\partial t^2}. \tag{A7}$$

We look for the so-called zero-phase solution of the form[21]

$$E(z, t) = \mathcal{E}(z, t)\cos\theta,$$
$$P(z, t) = S(z, t)\sin\theta, \tag{A8}$$

where

$$\theta = kz - \nu t \equiv \nu[z/c - t]. \tag{A9}$$

Although more general solutions exist, this one represents a stable solution as shown in Ref. 21.

We make the usual slowly varying amplitude and phase approximation in which

$$\frac{\partial \mathcal{E}}{\partial z} \ll k\mathcal{E}; \quad \frac{\partial S}{\partial z} \ll kS ,$$

$$\frac{\partial \mathcal{E}}{\partial t} \ll \nu\mathcal{E}; \quad \frac{\partial S}{\partial t} \ll \nu S . \tag{A10}$$

In this case, (A7) reduces to

$$\frac{\partial \mathcal{E}}{\partial z} + c^{-1}\frac{\partial \mathcal{E}}{\partial t} + \kappa\mathcal{E} = \frac{\nu}{2c\epsilon_0} S(z, t) , \tag{A11}$$

where the loss/unit length is

$$\kappa = \sigma/2c\epsilon_0 . \tag{A12}$$

We must solve for the polarization $S(z, t)$.

By (A3), (A8), and (A9), we have

$$\rho_{ab}(t) = -(i\mathcal{P}/\hbar)\int_0^t dt'\, \mathcal{E}(t')[\rho_{aa}(t') - \rho_{bb}(t')]\cos(kz - \nu t')e^{-(i\omega - \Gamma_{ab})(t-t')} . \tag{A13}$$

If we make the usual rotating-wave approximation, this reduces to

$$\rho_{ab}(t) = -\frac{i\mathcal{P}}{2\hbar} e^{i\theta}\int_0^t dt'\mathcal{E}(t')[\rho_{aa}(t') - \rho_{bb}(t')]\, e^{-[i(\omega-\nu)+\Gamma_{ab}](t-t')} . \tag{A14}$$

We next put (A14) and its conjugate into (A5) and use (A8). We find that

$$P(z, t) = \frac{N\mathcal{P}^2}{\hbar}\int_{-\infty}^{\infty} d\omega\, \sigma(\omega)\int_0^t dt'\, e^{-\Gamma_{ab}(t-t')}\mathcal{E}(t')[\rho_{aa}(t') - \rho_{bb}(t')][\sin\theta\cos(\omega - \nu)(t - t') + \cos\theta\sin(\omega - \nu)(t - t')] . \tag{A15}$$

However, $\sigma(\omega)$ and $\rho_{\alpha\alpha}(z, t, \omega)$ are even functions of $(\omega - \nu)$ so that the last term vanishes. Comparison then of (A15) and (A8) shows that

$$S(z, t) = \frac{N\mathcal{P}^2}{\hbar}\int_{-\infty}^{\infty} d\omega\, \sigma(\omega)\int_0^t dt'\, e^{-\Gamma_{ab}(t-t')}\mathcal{E}(t')[\rho_{aa}(t') - \rho_{bb}(t')]\cos(\omega - \nu)(t - t') . \tag{A16}$$

In order to proceed, it is convenient to define the quantities

$$\chi_{\alpha\alpha}(z, t, T) \equiv \int_{-\infty}^{\infty} d\omega\, \sigma(\omega)\rho_{\alpha\alpha}(z, t, \omega)\cos(\omega - \nu)T , \tag{A17}$$

where $\alpha = a, b$. Then $S(z, t)$ may be expressed as

$$S(z, t) = \frac{N\mathcal{P}^2}{\hbar}\int_0^t dt'\, e^{-\Gamma_{ab}(t-t')}\mathcal{E}(z, t')[\chi_{aa}(z, t', t - t') - \chi_{bb}(z, t', t - t')] . \tag{A18}$$

To obtain $\rho_{\alpha\alpha}$, we use (A14) and its adjoint and (A1) becomes

$$\frac{\partial \rho_{aa}}{\partial t} = r_a\delta\left(t - \frac{z}{c}\right) - \gamma_a\rho_{aa} - \frac{\mathcal{P}^2}{\hbar}\mathcal{E}(z, t)\cos\theta\int_0^t dt'\, e^{-\Gamma_{ab}(t-t')}\mathcal{E}(t')[\rho_{aa}(t') - \rho_{bb}(t')]\cos[\theta + (\omega - \nu)(t - t')] . \tag{A19}$$

We again make the rotating-wave approximation and obtain

$$\frac{\partial \rho_{aa}}{\partial t} = r_a\delta\left(t - \frac{z}{c}\right) - \gamma_a\rho_{aa} - \frac{\mathcal{P}^2}{2\hbar}\mathcal{E}(z, t)\int_0^t dt'\, e^{-\Gamma_{ab}(t-t')}\mathcal{E}(t')[\rho_{aa}(t') - \rho_{bb}(t')]\cos(\omega - \nu)(t - t') . \tag{A20}$$

Similarly, we find

$$\frac{\partial \rho_{bb}}{\partial t} = r_b\delta\left(t - \frac{z}{c}\right) - \gamma_b\rho_{bb} + \frac{\mathcal{P}^2}{2\hbar}\mathcal{E}(z, t)\int_0^t dt'\, e^{-\Gamma_{ab}(t-t')}\mathcal{E}(t')[\rho_{aa}(t') - \rho_{bb}(t')]\cos(\omega - \nu)(t - t') . \tag{A21}$$

Now from (A17) it follows that

$$\frac{\partial \chi_{\alpha\alpha}}{\partial t}(z, t, T) = \int_{-\infty}^{\infty} d\omega\, \sigma(\omega)\frac{\partial \rho_{\alpha\alpha}}{\partial t}\cos(\omega - \nu)T . \tag{A22}$$

If we use (A20) and the definitions (A17), we find

$$\frac{\partial \chi_{aa}}{\partial t} = r_a \delta\left(t - \frac{z}{c}\right) g(T) - \gamma_a \chi_{aa} - \frac{\mathcal{P}^2}{2\hbar}\, \mathcal{E}(t) \int_0^t dt'\, e^{-\Gamma_{ab}(t-t')}\, \mathcal{E}(t')$$

$$\times \int_{-\infty}^{\infty} d\omega\, \sigma(\omega)[\rho_{aa}(z, t', \omega) - \rho_{bb}(z, t', \omega)] \cos(\omega - \nu)(t - t') \cos(\omega - \nu) T \,. \tag{A23}$$

Here we have let

$$g(T) \equiv \int_{-\infty}^{\infty} d\omega\, \sigma(\omega) \cos(\omega - \nu) T = e^{-[(\Delta\omega_D T)^2/16 \ln 2]} \,, \tag{A24}$$

where we used (A6). If we use the identity

$$\cos A \cos B = \tfrac{1}{2}\cos(A + B) + \tfrac{1}{2}\cos(A - B)$$

and the definitions (A17), (A23) may be written

$$\frac{\partial \chi_{aa}}{\partial t} = r_a \delta\left(t - \frac{z}{c}\right) g(T) - \gamma_a \chi_{aa} - \frac{\mathcal{P}^2}{4\hbar}\, \mathcal{E}(t) \int_0^t dt'\, e^{-\Gamma_{ab}(t-t')}\, \mathcal{E}(t')$$

$$\times [\chi_{aa}(t', T + t - t') + \chi_{aa}(t', T - t + t') - \chi_{bb}(t', T + t - t') - \chi_{bb}(t', T - t + t')] \,. \tag{A25}$$

The equation for χ_{bb} is obtained by simply interchanging a and b everywhere in (A25).

We next linearize (A25). Then we have for $\alpha = a, b$,

$$\frac{\partial \chi_{\alpha\alpha}}{\partial t} + \gamma_\alpha \chi_{\alpha\alpha} = r_\alpha \delta\left(t - \frac{z}{c}\right) g(T) \,. \tag{A26}$$

The solution is easily verified to be

$$\chi_{\alpha\alpha}(z, t, T) = r_\alpha g(T) e^{-\gamma_\alpha \xi} u(\xi) \,, \tag{A27a}$$

where

$$\xi \equiv t - z/c \,, \tag{A27b}$$

and

$$u(\xi) = \begin{cases} 1 & \text{for } \xi > 0 \\ 0 & \text{for } \xi < 0 \,. \end{cases} \tag{A27c}$$

We next substitute (A27) into (A18), which is the driving term in (A11). We then multiply both sides of (A11) by $\mathcal{E}(z, t)$ to obtain

$$\left(\frac{\partial}{\partial z} + c^{-1}\frac{\partial}{\partial t} + 2\kappa\right) \mathcal{E}^2(z, t) = (\nu N \mathcal{P}^2/\hbar c \epsilon_0) \mathcal{E}(z, t)$$

$$\times \int_0^t dt'\, e^{-\Gamma_{ab}(t-t')}\, \mathcal{E}(z, t')[r_a e^{-\gamma_a(t'-z/c)} - r_b e^{-\gamma_b(t'-z/c}] g(t - t') u(t' - z/c) \,. \tag{A28}$$

Due to the presence of the unit step function, the lower limit on the t' integral becomes z/c. Also, if we let

$$\tau = t - t' \,, \tag{A29}$$

then (A28) becomes

$$\left(\frac{\partial}{\partial z} + c^{-1}\frac{\partial}{\partial t} + 2\kappa\right) \mathcal{E}^2(z, t) = (\nu N \mathcal{P}^2/\hbar c \epsilon_0) \mathcal{E}(z, t) e^{\beta^2}$$

$$\times u(\xi) \int_0^\xi d\tau\, \mathcal{E}(z, t - \tau)\{r_a e^{-\gamma_a \xi} e^{-\alpha(\tau - \beta/\alpha^{1/2})^2} - r_b e^{-\gamma_b \xi} e^{-\alpha(\tau + \beta/\alpha^{1/2})^2}\} \,. \tag{A30}$$

Here we have also used (A24) and let

$$\beta = (\ln 2)^{1/2}(\gamma_a - \gamma_b)/\Delta\omega_D \,,$$

$$\alpha = (\Delta\omega_D)^2/16 \ln 2 \,. \tag{A31}$$

We have also let $\Gamma_{ab} = \frac{1}{2}(\gamma_a + \gamma_b)$.

If we finally make the rate-equation approximation $\mathcal{E}(z, t - \tau) \to \mathcal{E}(z, t)$, then (A30) becomes

$$\left(\frac{\partial}{\partial z} + c^{-1}\frac{\partial}{\partial t} + 2\kappa\right) \mathcal{E}^2(z, t) = \frac{3}{2}\left(\frac{\ln 2}{\pi}\right)^{1/2} \lambda^2 \frac{\Delta\omega_S}{\Delta\omega_D} N \mathcal{E}^2(z, t) e^{\beta^2} u(\xi)\{r_a e^{-\gamma_a \xi} I_a - r_b e^{-\gamma_b \xi} I_b\} \,, \tag{A32}$$

where

$$I_a \equiv 2\left(\frac{\alpha}{\pi}\right)^{1/2}\int_0^\infty e^{-\alpha(\tau-\beta/\alpha^{1/2})^2}d\tau\ ,$$
$$I_b \equiv 2\left(\frac{\alpha}{\pi}\right)^{1/2}\int_0^\infty e^{-\alpha(\tau+\beta/\alpha^{1/2})^2}d\tau\ , \tag{A33}$$

and τ_S, the spontaneous lifetime, is given by

$$\Delta\omega_S \equiv \tau_S^{-1} = (\omega/c)^3\mathcal{O}^2/3\pi\hbar\epsilon_0\ . \tag{A34}$$

We have also used (A31) and have extended the upper limits in (A33) to infinity since the exponential decays rapidly. We may rewrite I_a and I_b as

$$I_a = 1+\mathrm{erf}\beta,\quad I_b = 1-\mathrm{erf}\beta\ . \tag{A35}$$

The solution of (A32) is

$$\mathcal{E}^2(z,\xi) = \mathcal{E}^2(0,\xi)\exp\left[\frac{3}{2}\left(\frac{\ln 2}{\pi}\right)^{1/2}\lambda^2\ \frac{\Delta\omega_S}{\Delta\omega_D}N[u(\xi)(r_a c^{-\gamma_a\xi}J_a - r_b e^{-\gamma_b\xi}J_b)] - 2\kappa\right]z\ , \tag{A36}$$

where

$$J_a \equiv e^{\beta^2}(1+\mathrm{erf}\beta),\quad J_b \equiv e^{\beta^2}(1-\mathrm{erf}\beta)\ . \tag{A37}$$

Thus, the net linear gain coefficient in a length l at time $t=z/c$ is

$$G = \left[\frac{3}{2}\left(\frac{\ln 2}{\pi}\right)^{1/2}\lambda^2\ \frac{\Delta\omega_S}{\Delta\omega_D}N(r_a J_a - r_b J_b) - 2\kappa\right]l\ . \tag{A38}$$

For our case, $r_b \ll r_a$. If we use (2.1), then

$$G \cong \left[\frac{3}{4}\left(\frac{\ln 2}{\pi}\right)^{1/2}\lambda^2\ \frac{\Delta\omega_S e^{\beta^2}(1+\mathrm{erf}\beta)i\Delta P}{\Delta\omega_D e v_0 \Delta x\Delta y} - 2\kappa\right]l\ . \tag{A39}$$

In the event $\beta \ll 1$, (A38) reduces to

$$G = \left[\frac{3}{4}\left(\frac{\ln 2}{\pi}\right)^{1/2}\lambda^2\ \frac{\Delta\omega_S i\Delta P}{\Delta\omega_D e v_0\Delta x\Delta y} - 2\kappa\right]l\ . \tag{A40}$$

*Work supported by the Advanced Research Projects Agency, and U.S. Army Research Office-Durham.

†Permanent address: Dept. of Physics and Electrical Engineering, University of Southern California, Los Angeles, Calif. 90007.

‡Alfred P. Sloan Fellow.

§Present address: Dept. of Physics, University of Alabama, Huntsville, Ala. 35807.

[1]A preliminary account of the present work was published in Opt. Commun. 9, 246 (1973). For a review of progress through April 1972, see R. C. Elton, R. W. Waynant, R. A. Andrews, and M. H. Reilly, NRL Report No. 7412, 2 May 1972 (unpublished), and references therein. In addition to the efforts as listed in Refs. 2–4, we wish to call attention to the following papers: M. A. Duguay and P. M. Rentzepis, Appl. Phys. Lett. 10, 350 (1967); P. Jaegle, A. Carillon, P. Dhez, G. Jamelot, A. Sureau, and M. Cukier, Phys. Lett. A 36, 167 (1971); T. C. Bristow, M. J. Lubin, J. M. Forsyth, E. B. Goldman, and J. M. Soures, Opt. Commun. 5, 315 (1972); H. Mahr and U. Roeder, Opt. Commun. 10, 227 (1974).

[2]B. Lax and A. Guenther, Appl. Phys. Lett. 21, 361 (1972).

[3]J. G. Kepros, E. M. Eyring, and S. W. Cagle, Jr., Proc. Natl. Acad. Sci. USA 69, 1744 (1972).

[4]R. A. McCorkle, Phys. Rev. Lett. 29, 982 (1972); and 29, 1428 (1972).

[5]M. Nunogaki, J. Itoh, H. Akimune, and T. Suita, Jpn. J. Appl. Phys. 10, 1640 (1971); Y. Okamoto and H. Tamagawa, Rev. Sci. Instrum. 43, 1172 (1972); R. C. Davis, O. B. Morgan, L. D. Stewart, and W. L. Stirling, *ibid.* 43, 278 (1972). In a duoplasmatron, singly ionized helium is accelerated to a high voltage where it collides with a target to produce He^{++}. An alternative scheme which would reduce the beam-velocity spread due to multiple scattering in the target would be to bombard the He^+ ions with a high-intensity laser to produce He^{++} ions.

[6]The authors wish to thank Dr. K. Boyer and Dr. J. E. Brolley of Los Alamos Scientific Labs for helpful discussion on this point [J. E. Brolley, IEEE Trans. Nucl. Sci. 20, 475 (1973)].

[7]H. Bethe and E. E. Salpeter, Handb. Phys. 35, 352 (1957).

[8]*Note added in manuscript:* Recent experimental work of the Yale group supports the conclusion of the present paper. In particular, our predicted population inversion of ≈5% is in reasonable agreement with their results for both atomic- and molecular-hydrogen targets [G. Khayrallah (private communication)]. The authors wish to thank Professor J. Bayfield and Dr. G. Khayrallah for helpful discussion and for making their results available before publication.

[9]R. Emigh (private communication).

[10]J. A. R. Samson, *Advances in Atomic and Molecular Physics*, edited by D. R. Bates and I. Estermann (Academic, New York, 1966), Vol. 2.

[11]R. Barnas, J. Phys. Radium 14, 34 (1953); and R. Barnas, L. Kalusyzner, and J. Druax, *ibid.* 15, 273 (1954).

[12]M. B. McElroy, Proc. R. Soc. Lond. A 272, 542 (1963). The cross section for electron pickup in the 2*s* state is comparable to that in 2*p*. We have neglected the effect of collisional transfer from $2s \rightarrow 2p$ since it is felt that this can only help us. Such processes will be discussed in a future publication.

[13]J. P. Coleman and M. R. C. McDowell, Proc. Phys. Soc. Lond. 83, 907 (1964).
[14]H. Schiff, Can. J. Phys. 32, 393 (1954).
[15]N. F. Mott and H. S. W. Massey, *The Theory of Atomic Collisions*, 3rd ed. (Oxford U. P., Oxford, 1965).
[16]W. L. Fite, A. C. H. Smith, and R. F. Stebbings, Proc. R. Soc. Lond. A 268, 527 (1962).
[17]T. F. Tuan and E. Gerjuoy, Phys. Rev. 117, 756 (1960).
[18]H. C. Brinkman and H. A. Kramers, Proc. Acad. Sci. Amst. 33, 973 (1930).
[19]J. D. Garcia (private communication).
[20]J. B. A. Stedeford, Proc. R. Soc. Lond. A 227, 466 (1955); S. K. Allison, Rev. Mod. Phys. 30, 1137 (1958).
[21]W. E. Lamb, Jr., Phys. Rev. 134, A1429 (1964); F. A. Hopf and M. O. Scully, *ibid.* 179, 399 (1969). The gain derivation we present is believed necessary because, to our knowledge, no treatment of a δ-function traveling-wave pumping mechanism has been presented. Furthermore, our results differ from those obtained by an intuitive application of the usual gain expression; see, for example, F. A. Hopf, P. Meystre, M. O. Scully, and J. F. Seely (unpublished).
[22]W. S. Bickel (unpublished).